MODEL UPDATING USING UNCERTAIN EXPERIMENTAL MODAL DATA

Y. Govers[1] and M. Link[2]

[1]Deutsches Zentrum für Luft- und Raumfahrt (DLR), Institute of Aeroelasticity,
Bunsenstr. 10, 37073 Göttingen, Germany
Yves.Govers@DLR.de

[2]University of Kassel, Institute of Statics and Dynamics,
Mönchebergstr. 7, 34109 Kassel, Germany
link@uni-kassel.de

Keywords: Stochastic Finite Element Model Updating, Uncertainty, Modal Testing, Structural Dynamics.

Abstract: The propagation of parameter uncertainty in structural dynamics has become a feasible method to determine the probabilistic description of the vibration response of industrial scale finite element models. Though methods for uncertainty propagation have been developed extensively, the quantification of parameter uncertainty has been neglected in the past. But a correct assumption for the parameter variability is essential for the estimation of the uncertain vibration response. This paper shows how to identify model parameter means and covariance matrix from uncertain experimental modal test data. The common gradient based approach from deterministic computational model updating was extended by an equation that accounts for the stochastic part. In detail an inverse approach for the identification of statistical parametric properties will be presented which will be applied on a numerical model of a replica of the GARTEUR SM-AG19 benchmark structure. The uncertain eigenfrequencies and mode shapes have been determined in an extensive experimental modal test campaign where the aircraft structure was tested repeatedly while it was 130 times dis- and reassembled in between each experimental modal analysis.

1 INTRODUCTION

The physical behaviour of structures is usually simulated by finite element (FE) models. The accuracy of each numerical model is dependent on correct modelling assumptions. However, a comparison between numerical output and test data from the real structure is necessary to verify a FE model. If the deviation between test and analysis exceeds required thresholds, the numerical model has to be adjusted to give a better representation of the physical behaviour for further calculations. Model updating methods in structural dynamics have been developed and improved for more than 30 years and they are widely used for fitting analytical models to real life structures. In current computational model updating methods, numerical results are adjusted to a single set of experimental data by optimising a preselected design parameter set. The effectiveness but also the limits of these methods have been studied comprehensively in the past (see for example [1], [2] or [3]). Different types of objective functions have been defined using input residuals, output residuals, (see [2]) or the error in the constitutive relation (see [4]). Even though deterministic methods achieve fairly good results by minimising the test/analysis deviation, the identified parameters are nevertheless deterministic. But, measurement data like modal data are always exposed to uncertainty. There exist several sources which

cause variability in the experimental modal analysis chain. Just to mention a few: human operator, modal identification algorithm, measurement noise, structure variability due to production tolerances etc. A previous study from [5] discusses the effect of different sources of variability in modal testing. This work showed, that a dominant source of variability even originates from disassembly and reassembly of a single test structure.
Hence, a stochastic model updating approach is needed to capture uncertainty in experimental modal data which includes following steps. Take modal test data with given statistical properties (*means* and *covariances* of eigenfrequencies, mode shape vectors, etc.) and identify the statistical properties of the uncertain model parameters. First approaches have been made in [6] covering the uncertainty in modal test data originating from measurement errors. Recent work presented in [7], [8], [9] and [10] address uncertainty related to production tolerances.
References [7] and [8] use the approach of [6] for the identification of stochastic model parameters from uncertain test data originating from variability amongst nominal identical structures. The work in [6] was based on measurement errors in modal data of a single test piece. Therefore the *covariances* of the identified stochastic parameters represent the confidence on the adjusted parameters in combination with the quality of the measurements. Consequently, this approach is not feasible to cover uncertainty related to production tolerances.
In references [9] and [10] an improved perturbation method for stochastic finite element model updating is applied where two recursive systems of equations for the adjustment of parameter *means* and *covariances* are derived. In [11] the author presents an interval model updating method which is also capable to identify model parameter uncertainty from statistical test data.
Here, a different approach for stochastic model updating will be presented. The classical model updating technique with a gradient based iteration procedure is extended by an equation accounting for the statistical properties. At first, the parameter *means* are updated by minimising the difference between test and analysis output *means* (*e.g.* frequency, mode shape deviations, etc.). Next, the parameter *covariance* matrix is adjusted by minimising the difference between test and analysis output *covariance* matrices based on their Frobenius norm.
This technique has first been proven on a simple three degree of freedom example as described in [12] and afterwards been applied to numerical case study with 15.000 degrees of freedom [13] on a generic aircraft model. Later on the developed method was applied for the adjustment of rigid body modes from real test data [14].

2 THEORETICAL BACKGROUND

2.1 Random variables

If a random variable x_j is sampled n times, the sample *mean* value is calculated from

$$\bar{x}_j = \frac{1}{n} \sum_{i=1}^{n} x_{ji}, (j = 1, \ldots, m) \tag{1}$$

where m denotes the number of random variables and the bar placed above any random variable indicates the average value. The *mean* values are assembled in the vector

$$\{\bar{x}\}^T = \langle\ \bar{x}_1 \quad \bar{x}_2 \quad \dots \quad \bar{x}_j \quad \dots \quad \bar{x}_m\ \rangle \tag{2}$$

The sample *covariance* between two random variables x_j and x_k which describes the second moment of correlation is calculated from

$$\mathbf{Cov}(x_j, x_k) = \frac{1}{n-1} \sum_{i=1}^{n} (x_{ji} - \bar{x}_j)\,(x_{ki} - \bar{x}_k) \tag{3}$$

and consequently the *covariance* matrix for a set of random variables x_j can be written as

$$[S_x] = \begin{bmatrix} \mathbf{Var}(x_1) & \mathbf{Cov}(x_1, x_2) & \cdots & \mathbf{Cov}(x_1, x_m) \\ \mathbf{Cov}(x_2, x_1) & \mathbf{Var}(x_2) & \cdots & \mathbf{Cov}(x_2, x_m) \\ \vdots & \vdots & \ddots & \vdots \\ \mathbf{Cov}(x_m, x_1) & \mathbf{Cov}(x_m, x_2) & \cdots & \mathbf{Var}(x_m) \end{bmatrix}, \tag{4}$$

where $\mathbf{Var}(x_j) = \mathbf{Cov}(x_j, x_j) = (\sigma(x_j))^2$ denotes the square of the *standard deviation* σ.

Because of the non-negative main diagonal and the symmetry, the *covariance* matrix is at least positive semi-definite. The *covariance* matrix can be normalised by the standard deviation which yields the correlation coefficient ρ

$$\rho(x_j, x_k) = \frac{\mathbf{Cov}(x_j, x_k)}{\sigma_{x_j} \sigma_{x_k}}. \tag{5}$$

The correlation coefficient between two random variables represents the statistical correlation and must always be in the range of $-1 \leq \rho \leq 1$. A graphical interpretation of the *covariance* between two random variables x and y can be given by the *covariance* ellipses as shown in figure 1. Here, the sample *mean* values and the *standard deviation* remain the same ($\bar{x} = \bar{y} = 0$ and $\sigma_x = \sigma_y = 1$), only the correlation coefficient ρ_{xy} (which is equal to the *covariance* in this case) between the two random variables is modified from -1 to 1.

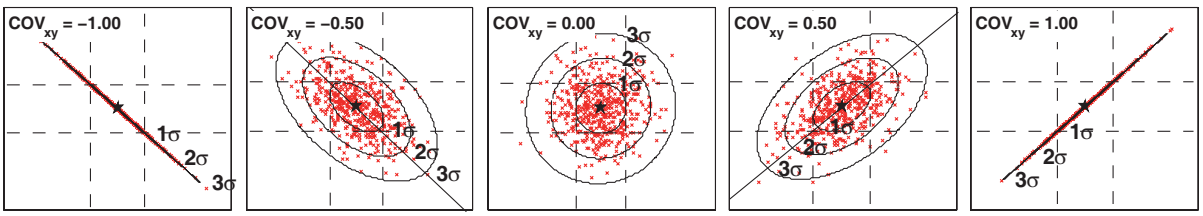

Figure 1: Covariance ellipses

It is clear from figure 1 that the two random variables x and y are completely dependent on each other when $\rho_{xy} = -1$ or 1. The cases in between represent a partial statistical

correlation of the two random variables. The ellipses represent contour lines of equal probability $p(x, y)$.

A linear transformation between two sets of random variables is expressed by

$$\{y\}_{(m\times 1)} = [C]_{(m\times n)}\{x\}_{(n\times 1)}, \tag{6}$$

where $[C]$ is the constant transformation matrix and $\{x\}, \{y\}$ are the vectors of random variables. The sample *mean* values $\{\bar{y}\}$ of a set of random variables $\{y\}$ can thus be expressed by the sample *mean* values $\{\bar{x}\}$ of the set of random variables $\{x\}$ using the same linear transformation

$$\{\bar{y}\}_{(m\times 1)} = [C]_{(m\times n)}\{\bar{x}\}_{(n\times 1)}. \tag{7}$$

Introducing this transformation into the *covariance* definition for the transformed variables $\{y\}$, $[S_y] = [\mathbf{Cov}(y, y)]$, yields

$$[S_y]_{(m\times m)} = [C]_{(m\times n)}[S_x]_{(n\times n)}[C]^T_{(n\times m)}. \tag{8}$$

2.2 Parameter estimation

The aim of parameter estimation techniques in the field of structural dynamics is to fit results of an analytical model as close as possible to the results obtained from an experiment. The real structural behaviour can be estimated by experimental modal analysis (EMA). Nevertheless test data is unavoidably polluted with random and systematic errors and therefore the adjusted parameters of the computer model are also estimated values. In case of uncertainty in the experimental data with known output *means* and *covariances* the parameter adjustment process can be split up into two independent recursive sets of equations.

1. *Mean parameter adjustment*: In the first step the *means* of the model parameters are updated by minimising the difference between the *means* of the measured and analytical output using a weighted least squares optimisation algorithm.
2. *Parameter covariance matrix adjustment*: In the second step the model parameter *covariance* matrix is updated by minimising the difference between the measured and analytical output *covariance* matrix using the Frobenius norm.

2.2.1 Mean parameter adjustment

The most important estimation technique for practical applications is the method of the weighted least squares. The parameter estimation starts by defining a residual which contains the differences between the analytical and measured results *e.g.* the difference between analytical and measured (*i.e.* 'estimated') eigenfrequencies.

If $\{\bar{v}_m\}$ is a vector containing the measured (subscript m) *mean* values and $\{\bar{v}_a(p)\}$ is the corresponding analytical (subscript a) *mean* vector which is a function of the *mean*

parameters to be updated, the error can be assembled in the weighted residual vector $\{\bar{\varepsilon}_w\}$

$$\{\bar{\varepsilon}_w\} = [W_v](\{\bar{v}_m\} - \{\bar{v}_a(p)\}), \tag{9}$$

with a suitable diagonal weighting matrix $[W_v]$. The values for the weighting matrix $[W_v]$ should be chosen with knowledge about the accuracy of the test data. Consequently the engineering judgement of the test engineer and the information about the reliability of the experimental modal data is absolutely essential. The method of the weighted least squares leads to the objective function for *mean* parameter adjustment

$$J = \{\bar{\varepsilon}_w\}^T\{\bar{\varepsilon}_w\} = \{\bar{\varepsilon}\}^T[W_\varepsilon]\{\bar{\varepsilon}\} \rightarrow \min \tag{10}$$

with $[W_\varepsilon] = [W_v]^T[W_v]$.

The minimisation of the squared sum of the weighted residual vector permits to estimate the updating parameters. The solution of the minimisation problem of equation (10) usually leads to a non-linear set of equations because $\{\bar{v}_a(p)\}$ is in general non-linearly dependent on the updating parameters. If we consider for example the height h of a beam as an update parameter, then the mode shapes are a non-linear function of h. Consequently, the residual vector, which *e.g.* contains the difference between the measured and analytical mode shapes, also depends in a non-linear way on h. In practical applications the non-linear optimisation problem is solved by expanding the analytical vector in a linearised Taylor series so that the objective function can be solved iteratively. The Taylor series truncated after the linear term is given by

$$\{\bar{v}_a(p)\}_{i+1} = \{\bar{v}_a\}_i + [G]_i\{\Delta\bar{p}\}_i, \tag{11}$$

where $\{\bar{v}_a\}_i$ represents the *mean* vector of the analytical response at the iteration step i, $[G]_i = \frac{\partial\{\bar{v}_a\}}{\partial\{\bar{p}\}}|_i$ represents the sensitivity (gradient) matrix of the size $(m \times n_p)$ (with $m =$ no. of measurements, $n_p =$ no. of estimation parameters) and $\{\Delta\bar{p}\}_i = \{\bar{p}\}_{i+1} - \{\bar{p}\}_i$ represents the vector of the *mean* parameter changes (increments) between successive iteration steps. Introducing equation (11) in equation (10) yields the linearised residual

$$\{\bar{\varepsilon}_w\}_i = [W_v](\{\bar{r}\}_i - [G]_i\{\Delta\bar{p}\}_i), \tag{12}$$

with $\{\bar{r}\}_i = \{\bar{v}_m\} - \{\bar{v}_a\}_i$. The vector $\{\bar{r}\}_i$ contains the residual between the test data and the model at the linearisation point of the i^{th} iteration step. The minimum of the objective function can be obtained from the condition $\frac{\partial J}{\partial\{\Delta\bar{p}\}} = 0$, which yields the linear set of equations by using the pseudo-inverse of the weighted sensitivity matrix $[W_v][G]_{(m\times n_p)}$ where $m > n_p$ (overdetermined system)

$$\{\Delta\bar{p}\}_i = [T_\varepsilon]_i\{\bar{r}\}_i, \tag{13}$$

with the transformation matrix $[T_\varepsilon]_i = \left([G]_i^T[W_\varepsilon][G]_i\right)^{-1}[G]_i^T[W_\varepsilon]$.

In case of bad convergence properties because of an ill-conditioned sensitivity matrix the objective function J can be supplemented by a regularisation term that enforces small parameter changes $\Delta\bar{p}$

$$J = \{\bar{\varepsilon}\}^T[W_\varepsilon]\{\bar{\varepsilon}\} + \{\Delta\bar{p}\}^T[W_{p,\varepsilon}]\{\Delta\bar{p}\} \rightarrow \min. \tag{14}$$

The matrix $[W_p]$ can be derived from $[W_p] = w_p[B]$. In case of $[B] = [I]$ the additive term is equivalent to the classical Tikhonov regularisation [15]. A more sophisticated regularisation technique is described by using the inverse of the main diagonal of $([G]^T[W_\varepsilon][G])$ see [2], where $[B]_i$ is derived at every iteration step as follows:

$$[B]_i = \frac{\mathbf{Tr}([C]_i)}{\mathbf{Tr}([C]_i^{-1})}[C]_i^{-1}, \tag{15}$$

with matrix $[C]$ in MATLAB notation $[C]_i = diag\left(diag\left([G]_i^T[W_\varepsilon][G]_i\right)\right)$.

This regularisation technique is adaptive in each iteration step because it is related to the inverse of the squared sensitivity matrix which changes from step to step. With this extension the minimisation of the extended objective function leads to the transformation matrix

$$[T_\varepsilon]_i = \left([G]_i^T[W_\varepsilon][G]_i + [W_{p,\varepsilon}]_i\right)^{-1}[G]_i^T[W_\varepsilon]. \tag{16}$$

2.2.2 Parameter covariance matrix adjustment

If $[S_{v_m}]$ is the *covariance* matrix of the measured samples and $[S_{v_a(p)}]$ is the corresponding analytical *covariance* matrix which is a function of the *covariance* matrix of the parameters to be updated, the error can be summarised in a residual matrix $[S_\Delta]$

$$[S_\Delta]_i = [S_{v_m}] - [S_{v_a(p)}]_i, \tag{17}$$

with a suitable diagonal weighting matrix $[W_S]$ (which should be chosen in the same way as $[W_v]$) we can formulate the following objective function for the *covariance* matrix adjustment

$$J_S = \frac{1}{2}\left\|[W_S][S_\Delta][W_S]^T\right\|_F^2 \rightarrow \min, \tag{18}$$

by using the definition of the Frobenius norm of a matrix $[A]_{(r\times s)}$

$$\|[A]\|_F^2 \;=\; \sum_{j=1}^{r}\sum_{k=1}^{s}|a_{jk}|^2 = \mathbf{Tr}([A]^H[A]). \tag{19}$$

The Taylor series expansion of the analytical output *covariance* matrix $[S_{v_a(p)}]$ truncated after the first linear term leads to

$$\begin{aligned}[S_{v_a(p)}]_{i+1} &= \left[\,\mathbf{Cov}\left(\{v_a\}_i + [G]_i\{\Delta p\}_i, \{v_a\}_i + [G]_i\{\Delta p\}_i\right)\right] \\ &= [S_{v_a}]_i + [G]_i[S_{\Delta p}]_i[G]_i^T,\end{aligned} \tag{20}$$

with the assumption that $\{v_a\}_i$ and $\{\Delta p\}_i$ are uncorrelated. This assumption is true for the first updating step but an approximation for any other iteration step.

The matrix $[S_{\Delta p}]_i$ denotes the system parameter *covariance* matrix changes (increments) with $[S_{\Delta p}]_i = [S_p]_{i+1} - [S_p]_i$ where $\{p\}_{i+1}$ and $\{p\}_i$ are also assumed to be uncorrelated. $[G]_i$ represents the sensitivity matrix at the i_{th} iteration step which is obtained in the same way as for equation (11). Therefore the residual *covariance* matrix $[S_\Delta]$ can be expressed as

$$[S_\Delta]_i = [R]_i - [G]_i[S_{\Delta p}]_i[G]_i^T, \tag{21}$$

with $[R]_i = [S_{v_m}] - [S_{v_a}]_i$,

where $[S_{v_a}]_i$ represents the *covariance* matrix of the analytical response at the iteration step i. Minimising the objective function J_S using the condition $\frac{\partial J_S}{\partial [\Delta S_p]} = 0$ leads to the equation

$$[S_{\Delta p}]_i = [T_\Sigma]_i\ [R]_i\ [T_\Sigma]_i^T, \tag{22}$$

where $[T_\Sigma]_i = \left([G]_i^T[W_\Sigma][G]_i\right)^{-1}[G]_i^T[W_\Sigma]$ represents the transformation matrix at the i^{th} iteration step, which is the same as in equation (13) except the weighting matrix $[W_\Sigma] = [W_S]^T[W_S]$. The detailed derivation of this equation can be found in [12].

In case of an ill-conditioned sensitivity matrix $[G]$ the inverse of the matrix product $([G]^T[W_\Sigma][G])$ can be extended by an additive regularisation term $[W_p]$ to improve the convergence. In this case the extended transformation matrix $[T_\Sigma]$ is written as

$$[T_\Sigma]_i = \left([G]_i^T[W_\Sigma][G]_i + [W_{p,\Sigma}]_i\right)^{-1}[G]_i^T[W_\Sigma]. \tag{23}$$

A suitable regularisation matrix $[W_{p,\Sigma}]$ can be derived as shown in equation (15).

2.3 Residual type

The updating process is split into two independent equations. For this reason the residual can be different for parameter *means* and *covariances*. Since the first equation represents the classical updating the typical frequency, mode shape and modal assurance criterion (MAC) residual or a weighted combination of two or three residuals can be chosen. Here,

parameter *means* will be updated by frequency and mode shape residual as described in [2]. The parameter *covariance* matrix is adjusted by the frequency *covariance* matrix residual only which results in minimising the difference between test and analysis frequency scatter (*covariance*) ellipses as presented in figure 1.

2.4 Sampling method

To derive the statistical finite element solution the Monte Carlo method has been taken using a multivariate normal distribution. Since simple random sampling is very time consuming Latin Hypercube Sampling (LHS) has been introduced to reduce the number of samples in an efficient way while gaining stability in the optimisation process. LHS can shortly be described for uncorrelated random variables as follows:

- divide the cumulative distribution into N equiprobable intervals,
- select a value from each interval randomly,
- transform the probability values by the inverse of the distribution function,
- derive a multivariate distribution by pairing the variables randomly.

In case of correlated random variables LHS is based on the Cholesky decomposition as proposed in [16]. Figure 2 underlines the efficiency of LHS in contrast to simple random sampling. Here, the standard deviations are shown for *means* and *std* of varying sample sizes. Therefore every sample size was taken 1000 times. Subsequently the *means* and *std* values have been calculated. From these 1000 *mean* and *std* values again the *standard deviation* been determined and plotted in figure 2.

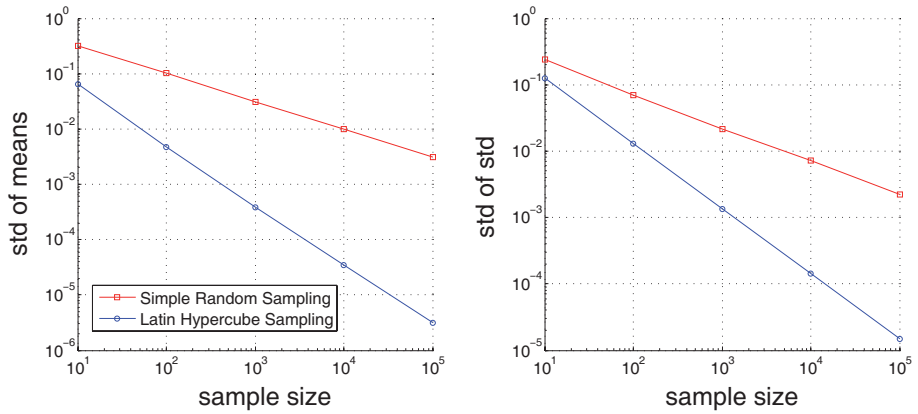

Figure 2: Comparison of sampling techniques

LHS already shows very little variability of the statistical properties at a sample size of $n = 100$ while the same variability using simple random sampling is reached not before taking a sample size that is two to three orders of magnitude higher.

3 UNCERTAINTY IN EXPERIMENTAL MODAL DATA

Uncertainty in experimental modal data may have manifold reasons. In detail: human operator, modal identification algorithm, measurement noise, structure variability due to production tolerances etc. This may all lead to a certain variability on the modal parameters. If serial production is considered the variation of material parameters, the accuracy

and repeatability of joint stiffness and damping parameters and production tolerances will affect the dynamical characteristics of the product. To capture and quantify all these effects on the modal parameters a representative test structure (see figure 3) was selected which is identical to the SM-AG19 model that was already subject to a pan-European study on experimental modal analysis. Back then, in 1995 the Action Group SM-AG19 was established by the Group for Aeronautical Research and Technology (GARTEUR) Executive Committee to analyse different test methods and to determine the variability in experimental modal data. For this reason, a benchmark structure was designed which should represent the structural behaviour of an aircraft. The test set-up was clearly defined in order to ensure a perfect structural repeatability. In the following the structure was analysed by twelve different test facilities of five European countries. Nevertheless, the experimental modal analysis results and even the frequency response functions (FRFs) from all participants showed significant discrepancies (see [17–19]).
Afterwards a benchmark study on validating different numerical models to a common set of measured data (European COST Action F3 on 'Structural Dynamics') was launched (see [20]). It was set up not only to compare the different computational model updating (CMU) procedures using a common test structure but also to see if the expected non-uniqueness of the results due to different computational methods, different structural idealisations and different parameter sets and, of course, different test data sets can be tolerated with regard to the intended utilisation.
So both has been present, uncertainty in the test data because of various test methods, boundary conditions, etc. of the different test facilities and uncertainty in the numerical models due to different updating techniques. But test data and computational model updating was more or less considered to be deterministic.
Here, the stochastic model updating approach will be shown on the replica of the GARTEUR SM-AG19 benchmark structure. This approach covers both at the same time.

3.1 Test set-up for case study of scatter sources

The examined test object (see figure 3) in the case study is a replica of the well known GARTEUR SM-AG19 structure. The replica is called **AIR**craft **MOD**el (AIRMOD) and was built at DLR Göttingen to investigate concepts for Ground Vibration Testing (GVT). The overall structure is made of aluminium and consists of six beam like components connected by five bolted joints which are illustrated in figure 4. Its wing span amounts to 2.0 m, the length of the fuselage is 1.5 m and the height 0.46 m. The total weight of the structure adds up to 44 kg. Two additional masses of 300 gram each are installed at the forward tips of the winglets to ensure a better excitation of the wing torsion modes.

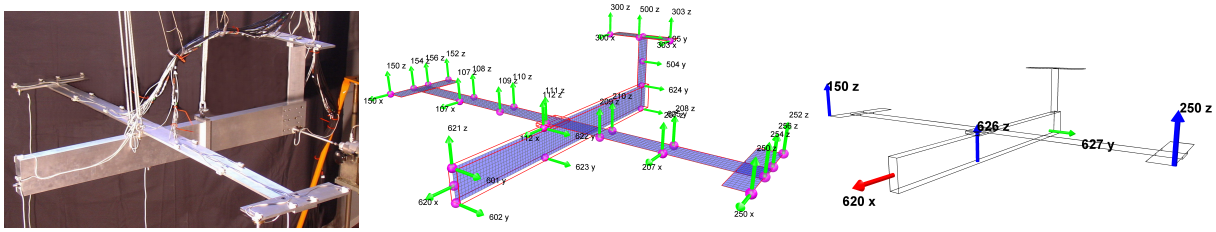

(a) Testbed (b) Measurement points on FEM (c) Exciter locations

Figure 3: AIRcraft MODel

To take account for reproducibility of the structural behaviour the joints were screwed

together with a torque control wrench and a predefined sequence for tightening the bolts of each joint. During the whole test series the set-up remained in the same configuration. All sensors and cables were just installed once in order to avoid further variability.

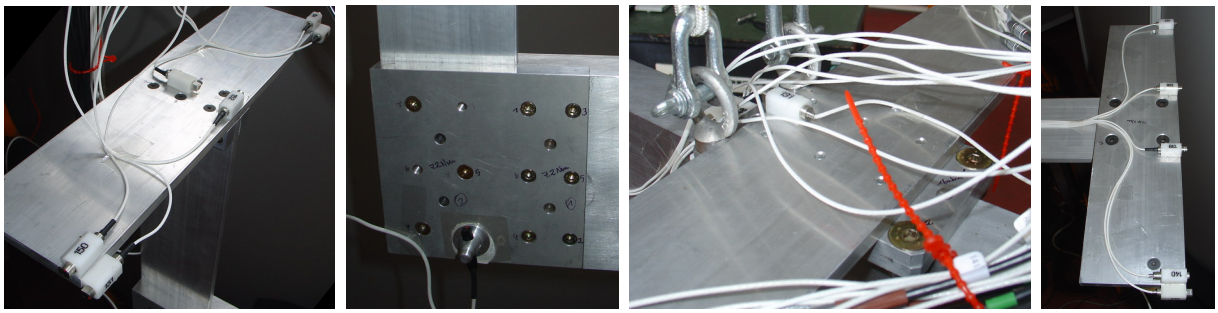

(a) VTP/HTP (b) VTP/fuselage (c) wing/fuselage (d) winglet

Figure 4: Bolted joints of AIRMOD

3.1.1 Boundary condition

The modal survey test series was carried out under the simulation of free-free boundary conditions. The support was realised by using a suspension with three soft bungee cords connected to a frame type structure. The assumption of free-free boundary conditions is satisfied by using a rule of thumb which says to separate the highest rigid body mode (RBM) from the first elastic mode of the structure by the factor $max(f_{RBM}) \approx 1/3 \cdot min(f_{elastic})$. The highest rigid body mode eigenfrequency was measured for the aircraft heave mode (RBM in vertical direction) at around 2Hz which was well separated from the first elastic mode (2n wing bending) at 5.5Hz. The bungee cords supporting the structure were relieved of the load out of the test phases to avoid an effect of relaxation and to keep the rigid body modes at an almost constant frequency level.

3.1.2 Sensor and exciter locations

The accelerometer locations were selected according to previous configurations of the GARTEUR benchmark. Therefore it was not necessary to conduct a pre-test analysis again. Nevertheless the sensor positions have been supplemented by a number of sensors to better visualise the mode shapes. Altogether 38 measurement points were defined. The sensor cables were also supported by the frame type structure to minimise the effect of additional mass loading and damping. The positions of the accelerometers are shown in figure 3b.
The exciter locations have been chosen in the same way. Five excitation points for hammer impact and shaker attachment have been selected as illustrated in figure 3c.

3.2 Analysis of sources for uncertainty in experimental modal data

At first the focus of the study was set on the quantification of the scatter of modal parameters due to well defined modifications in the modal analysis chain. During the whole test campaign the test set-up was not changed at all. The modifications which have been introduced are explained in the following:

1. *Scatter from hammer impact*
   For this scatter source the variability of modal parameters due to the analysis of

repeated samples of FRF sets recorded from hammer impact excitation was analysed. The discrepancies arise from multiple hammer impact tests performed without changing anything neither the structure nor the subsequent modal analysis with the PolyMAX algorithm implemented in LMS Test.Lab (see [21]). The hammer tests were executed by the same person at different days. For this test series 10 hammer impacts were chosen for averaging. Deviations shown here should represent the scatter of repeatability of hammer tests on AIRMOD.

2. *Reassembly scatter*
   A very important issue in serial production is the structural variability due to fabrication tolerances. In order to observe the variation of modal parameters from this source it was not possible to produce as many test structures as necessary for scatter analysis but reassembling the whole structure was found to be suitable to determine the variability in respect to serial production. Here, multiple hammer tests were performed by the same operator after complete reassembly of the structure with predefined sequences of steps using a torque control wrench for the bolted joints. Subsequently modal analysis was performed by the same person with the before mentioned software. During assembling and disassembling the structure the sensors were kept mounted in order to avoid further variability in the measurement data.
3. *Operator scatter*
   If different persons perform hammer testing on the same structure using an identical set-up the measured data will differ due to the individual execution of the hammer impacts. Furthermore, different philosophies for evaluating the experimental data will lead to even more spreading modal parameters when evaluated by different test personal. Therefore all members of the ground vibration test team at DLR Göttingen specialised on modal analysis acquired their own measurement data and subsequently performed the modal analysis as mentioned above.
4. *Analysis method scatter*
   Usually different modal analysis tools yield different results for the identified parameters. Therefore, discrepancies resulting from the extraction of modal parameters using different software codes were analysed. The parameter estimation was conducted with the same measurement data for the different codes.
5. *Sweep excitation scatter*
   Frequency response functions of linear structures should be independent to the force level used for excitation. Here differences in FRFs due to shaker excitation at different force levels and scatter of modal parameters of the subsequent modal analysis will be presented. In this case the force level amplitudes vary from 1 to 16N.
6. *Phase resonance method scatter*
   Testing large aircraft structures a test strategy is usually applied which makes use of a combination of phase resonance testing and phase separation techniques. In general, flutter critical modes are tuned via the phase resonance method whereas all the other modes are extracted with the phase separation method. This shows that the aircraft industry still believes more in modes obtained from phase resonance testing. Therefore the variability of modal parameters extracted from an excitation of the structure in steady state was analysed using different force levels between 1 and 16N.

The detailed results of this campaign have been shown in [22]. The variability of the test data due to some of the above mentioned test scatter sources is illustrated in figure 5. Here

the summed amplitudes of the measured frequency response functions show the impact of the chosen scatter source on the dynamical behaviour of the structure.

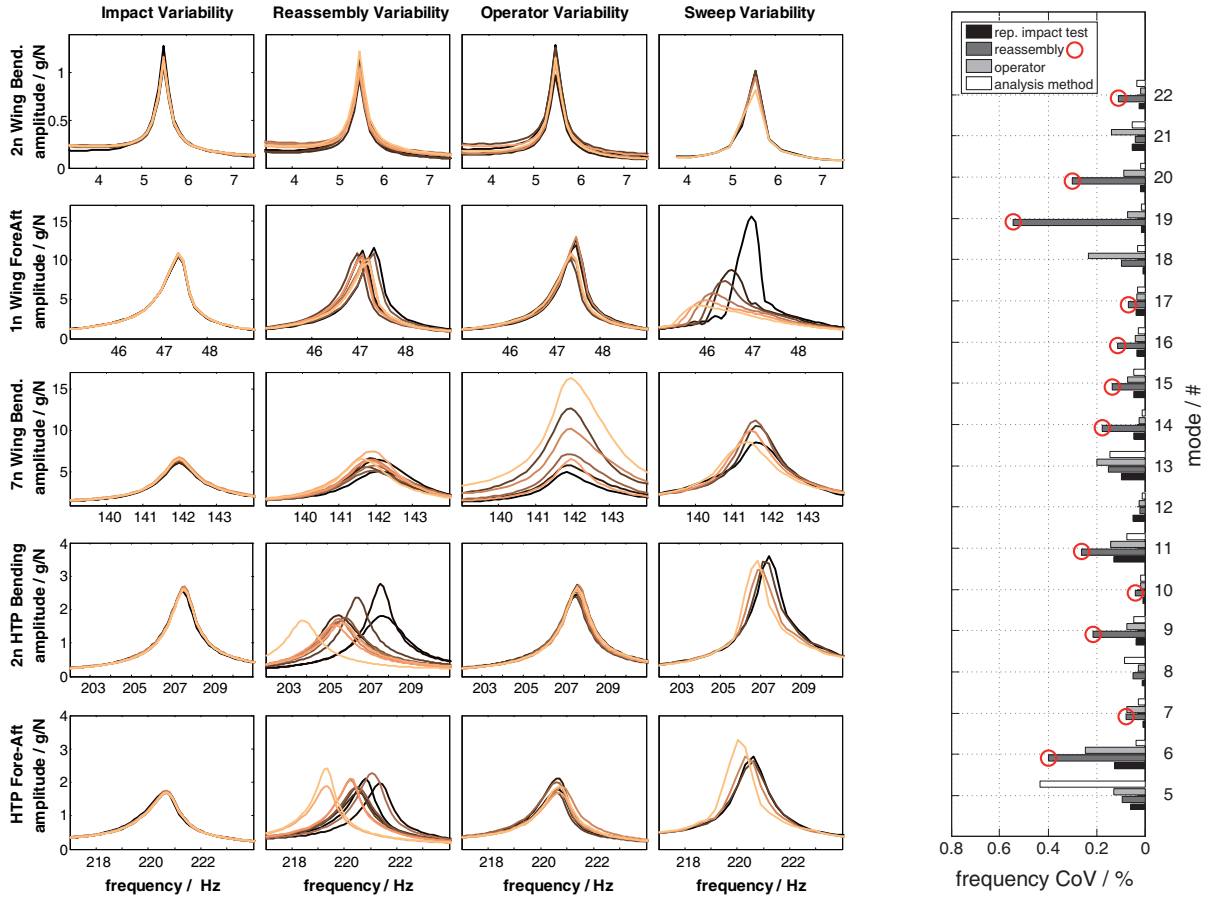

(a) FRF variation (b) Frequency variation

Figure 5: Variability for selected modes from different scatter sources

This study revealed that reassembling the structure has a significant impact on the eigen-frequency variability. Besides swept sine excitation on different force levels it shows the highest peak variation in the FRF's. While swept-sine testing on different force levels activates non-linear behaviour in the bolted joint connections it is not suited to represent stochastic effects. But reassembling and testing *e.g.* with random (low energy input) or even hammer impact excitation to just identify the linear behaviour was found to be the right method to gain a dataset with stochastic behaviour.

4 REPEATED MODAL SURVEY TEST BY REASSEMBLING THE JOINTS

To study the influence of reassembly on the scatter of modal parameters a test set-up was chosen where almost no user interaction was necessary. The structure was excited at two different exciter locations (626z and 627y, see figure 3c) using a random excitation signal in the frequency band from 0 to 400Hz. Time domain response data was recorded at the sensor locations shown in figure 3b with a sampling frequency of 1024Hz and a total length of 205sec. Frequency response functions were obtained using the Welch's method with an overlap of 90% and a block size of 16384. A hanning window was used to account for leakage effects when performing spectral analysis with the time data. These settings resulted in a frequency resolution of 0.031Hz. After complete disassembly of the

test structure the reassembly was conducted with predefined sequences of steps using a torque control wrench for the bolted joints. During the assembly and disassembly of the structure the accelerometers remained installed in order to avoid further variability in the measurement data. The structure was reassembled 130 times. This leads to 260 random tests using single point excitation.

4.1 Experimental modal parameter variability from reassembling

Subsequently modal analysis was performed on the 260 sets of frequency response functions with a MATLAB based in house software using the PolyMAX algorithm (see [21]). The experimental modal analysis procedure was fully automated based on a procedure that uses the automatic evaluation of the stabilisation charts. Here, also the MAC criterion has been used to identify double selection in combination with quality indicators like the modal phase collinearity (MPC) and the mean phase deviation (MPD) see [23]. Consequently, the effect of the operator during the parameter estimation process was eliminated and the algorithm based scatter was minimised.
After the modal identification each mode was only considered from a single exciter location. The decision was done from quality criteria (MPC and MPD) and basically resulted in taking symmetrical modes from exciter location 626z and anti-symmetrical modes from exciter location 627y. Unsymmetrical modes which appear in the higher frequency range above 250Hz have been chosen either from point 626 or 627. The separation between the exciter locations is also done to compare only modes of constant quality.

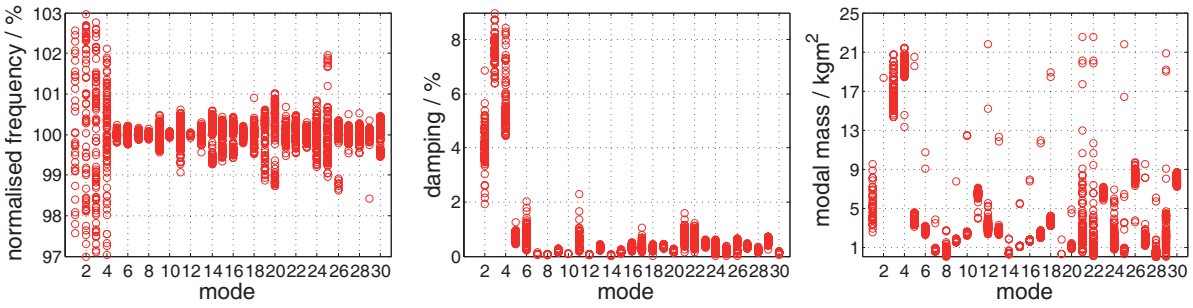

Figure 6: Modal data variation

To compare the modes that belong to the same shape they first have to be paired automatically by the modal assurance criterion and an additional frequency deviation threshold. Figure 6 shows the variability in the experimental modal parameters identified with the above mentioned procedure. The eigenfrequency has been normalised to 100 % for better comparison. It can be observed that the first 4 eigenfrequencies which refer to rigid body modes show quite a large variation by more than ±3% while the elastic modes 5 to 30 do not exceed the threshold of ±1.5%.
The complete frequency variation is listed in table 1. It also shows the frequency coefficient of variation f_{CoV} which is the frequency *standard deviation* divided by the *mean* value. It gives a good measure which modes are most affected by the reassembly. The last column shows the number of modes used for statistics. From 130 samples one sample was corrupted and a system change took place between sample 43 and 44. Therefore so only a maximum of 86 samples could be used. Nevertheless some modes have been identified less than 86 times which is due to the automatic identification and correlation process.

	mode name	f_{mean}/Hz	f_{std}/Hz	f_{CoV}/%	f_{min}/Hz	f_{max}/Hz	samples
01	RBM Yaw	0.23	0.006	2.41	0.22	0.24	41
02	RBM Roll	0.65	0.019	2.89	0.60	0.68	81
03	RBM Pitch	0.83	0.017	1.99	0.80	0.88	83
04	RBM Heave	2.17	0.024	1.11	2.11	2.22	86
05	2nWingBending	5.50	0.004	0.07	5.49	5.52	86
06	3nWingBending	14.91	0.017	0.12	14.88	14.94	86
07	WingTorsionAnti	31.96	0.020	0.06	31.92	32.01	86
08	WingTorsionSym	32.33	0.017	0.05	32.29	32.38	86
09	VtpBending	34.38	0.081	0.24	34.23	34.54	86
10	4nWingBending	43.89	0.015	0.03	43.85	43.92	86
11	1nWingForeAft	46.71	0.149	0.32	46.27	46.99	86
12	2nWingForeAft	51.88	0.012	0.02	51.84	51.91	86
13	5nWingBending	58.59	0.075	0.13	58.33	58.76	86
14	VtpTorsion	65.93	0.274	0.42	65.46	66.33	86
15	2nFuseLat	100.05	0.280	0.28	99.38	100.48	86
16	2nVtpBending	124.56	0.356	0.29	123.85	125.10	86
17	6nWingBending	129.38	0.107	0.08	129.12	129.66	86
18	7nWingBending	141.47	0.347	0.25	140.79	142.76	85
19	2nHtpBending	205.59	1.023	0.50	203.24	206.87	86
20	HtpForeAft	219.07	1.663	0.76	216.29	221.30	86
21	WingBendingRight	254.73	0.557	0.22	253.41	256.48	70

Table 1: Variability of identified eigenfrequencies

The variation of the mode shape vectors can also be determined. The *mean* mode shape has to be extracted iteratively by the following procedure since the shapes are usually scaled to unit modal mass or maximum component equal 1. Therefore take a reference mode $\{\phi_{j,ref}\}$ and calculate the modal scale factor (MSF) (see [24]) between sample k of mode j $\{\phi_{j,k}\}$ and the reference mode by

$$\mathbf{MSF}_j = (\{\phi_{j,k}\}^{\mathbf{T}}\{\phi_{j,k}\})^{-\mathbf{1}}\{\phi_{j,k}\}^{\mathbf{T}}\{\phi_{j,ref}\} \tag{24}$$

for all corresponding samples $k = 1 \ldots n$. Afterwards calculate the *mean* mode shape $\{\bar{\phi}_j\}$ using following equation.

$$\{\bar{\phi}_j\} = \frac{1}{n}\sum_{k=1}^{n}\mathbf{MSF}_j\{\phi_{j,k}\} \tag{25}$$

Then use the determined *mean* mode shape as a reference mode, calculate new MSF values and determine the *mean* mode shape again. Repeat this sequence until the *mean* shape does not change any more. When $\{\bar{\phi}_j\}$ is derived the standard deviation can be calculated component wise for each mode j. The result of this procedure is shown for modes 1 to 21 in figure 7. Gray cylinders at the sensor locations represent 2σ of the according mode shape amplitude. The largest *standard deviation* on amplitudes is found for modes 1,2 and 21.

5 PARAMETER MEAN AND COVARIANCE MATRIX IDENTIFICATION

5.1 Finite element model

The MSC.NASTRAN finite element model contains 2575 nodes, 2184 CQUAD4, 3 CROD, 77 CELAS1, 41 CONM1, 6 CMASS1, 39 RBAR, and 39 RBE2 elements. CQUAD4 elements are used to model the overall structure while CELAS1, CONM1 and RBE2 elements

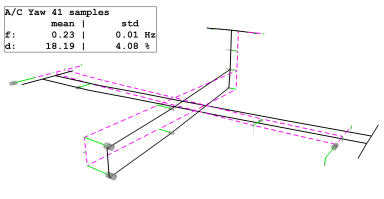

(a) 1 - RBM Yaw

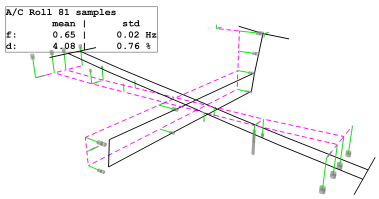

(b) 2 - RBM Roll

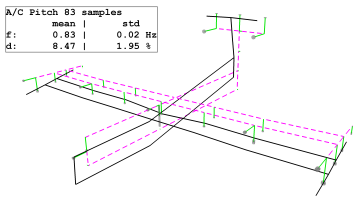

(c) 3 - RBM Pitch

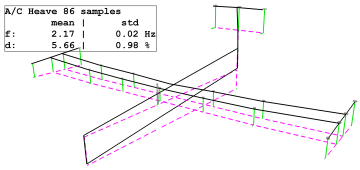

(d) 4 - RBM Heave

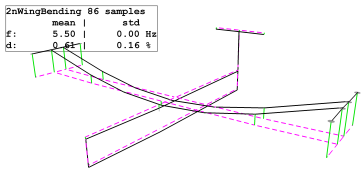

(e) 5 - 2n Wing Bending

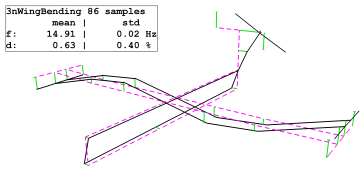

(f) 6 - 3n Wing Bending

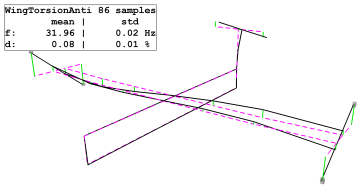

(g) 7 - Wing Torsion Anti.

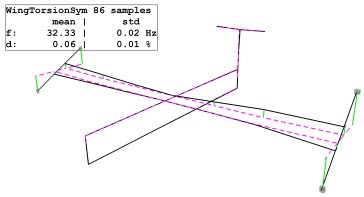

(h) 8 - Wing Torsion Sym.

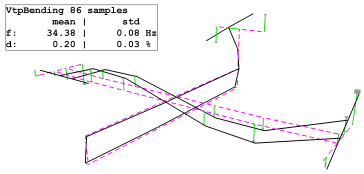

(i) 9 - VTP Bending

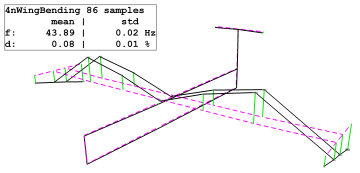

(j) 10 - 4n Wing Bending

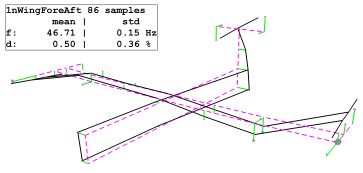

(k) 11 - 1n Wing in-plane Bend.

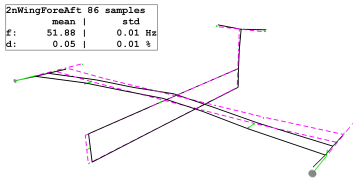

(l) 12 - 2n Wing in-plane Bend.

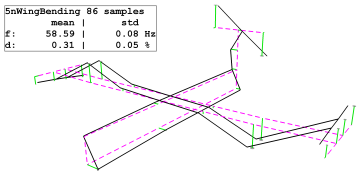

(m) 13 - 5n Wing Bending

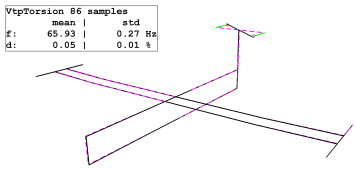

(n) 14 - VTP Torsion

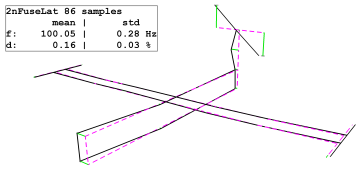

(o) 15 - 2n Fuselage Lateral Bend.

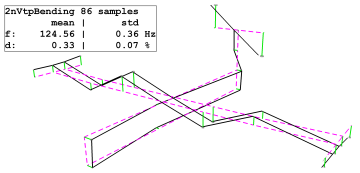

(p) 16 - 2n VTP Bending

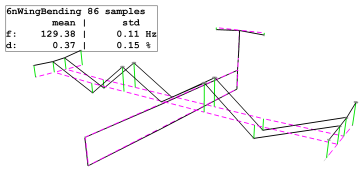

(q) 17 - 6n Wing Bending

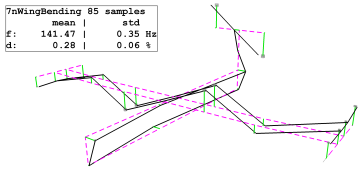

(r) 18 - 7n Wing Bending

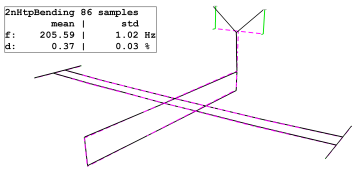

(s) 19 - 2n HTP Bending

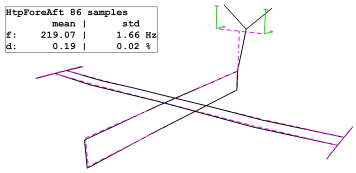

(t) 20 - HTP fore-aft Bending

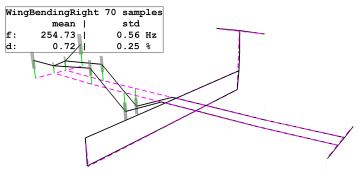

(u) 21 - Wing Bending Right

Figure 7: Mode shape amplitudes and its standard deviation of modes 1-21

are utilised to represent the details in the bolted connections (CELAS1, RBE2, RBAR) and additional mass loading by sensors and cables (CONM1, CMASS1). CELAS1 elements are used at the bolted connection of wing/fuselage in y-direction to account for a rotational spring around the z-axis. The same elements are placed at the VTP/HTP connection also in y-direction. At the VTP/fuselage joint two degrees of freedom are connected by springs: the z-translation and the x-rotation. Every sensor is represented by a CONM1 element of 15 gram and additional masses at the front part of the wing tips are also idealised by concentrated masses. The Monte Carlo Simulation was performed to determine the analytical *mean* results and *covariance* matrices with a sufficient number of samples ($n_{max} = 500$) using LHS.

5.2 Parameter selection and adjustment

The parameter estimation is shown for all identified rigid body modes and some of the elastic modes shown in figure 7. In detail modes no. 1 to 6, 14 and 19 have been chosen for the optimisation.
The bungee cords which can be seen in figure 3a have been modelled as CROD elements to constrain the vertical degrees of freedom. From this support the A/C Heave and A/C Pitch mode is already constrained. Since also A/C Roll and A/C Yaw could be identified from the test data additional spring elements have been introduced into the numerical model. A rotational spring at the wing fuselage connection accounts for the roll motion and two springs in y-direction (wing direction) represent the yaw/lateral stiffness. The springs were placed at locations where a bunch of cables was fixed to the structure.
Parameters for the adaptation of the elastic modes have been introduced at the wing/fuse joint and the HTP/VTP joint. Here stiffness and mass parameters have been selected. The final parameter selection has arisen from a large sensitivity study where more than 25 stiffness and mass parameters located at the joints and cable attachment points were analysed.
The updating parameters can therefore be described as follows:

- Parameter 1: stiffness of front suspension in z-direction,
- Parameter 2: stiffness of rear suspension in z-direction,
- Parameter 3: stiffness of roll motion by rotational spring k_{xx} at wing fuselage connection,
- Parameter 4: stiffness of yaw/lateral motion by spring at wing/fuselage connection in y-direction,
- Parameter 5: stiffness of HTP/VTP joint by translational springs k_y between connecting elements,
- Parameter 6: stiffness of HTP/VTP joint by Young's modulus of connecting elements,
- Parameter 7: mass at HTP/VTP joint to account for vibrating cable masses and
- Parameter 8: mass at WING/FUSE joint to account for vibrating cable masses.

All *mean* values of the parameters are adjusted together with the full *covariance* matrix. Updating was performed using small regularisation to the inverse of the sensitivity matrix as described in equation (15) with $w_{p,\varepsilon} = 0.025$ for the *mean* equation and $w_{p,\Sigma} = 0.04$ for the *covariance* matrix adjustment.

	f_{Mean} / Hz	Δf_{Mean} / %		f_{STD} / Hz	Δf_{STD} / %	
	EMA	FEM, ini.	FEM, upd.	EMA	FEM, ini.	FEM, upd.
01	0.23	-1.72	-0.00	0.006	-42.26	0.27
02	0.65	7.08	-0.01	0.019	-60.75	-2.34
03	0.83	-12.77	-0.00	0.017	-45.88	-0.06
04	2.17	-10.38	0.00	0.024	-8.55	-0.17
05	5.50	-0.04	-0.00	0.070	-35.45	0.24
06	14.91	-0.00	0.00	0.120	-18.76	-1.46
07	31.96	-0.42	-0.43	0.060	-71.24	-60.32
08	32.33	0.50	0.50	0.050	-99.20	-98.78
09	34.38	1.31	1.15	0.240	-83.37	-73.97
10	43.89	1.22	1.16	0.030	-76.77	-58.86
11	46.71	-2.37	-2.44	0.320	-95.05	-91.18
12	51.88	-3.06	-3.22	0.020	5.78	89.00
13	58.59	0.53	0.23	0.130	-56.62	-25.69
14	65.93	-3.59	-0.00	0.420	-50.46	1.36
15	100.05	-5.72	-5.13	0.280	-84.15	-68.95
16	124.56	-4.54	-4.17	0.290	-92.58	-83.68
17	129.38	-3.19	-3.20	0.080	-97.92	-96.29
18	141.47	-3.20	-2.89	0.250	-95.30	-86.69
19	205.59	-6.43	0.00	0.500	-53.58	-0.16
20	219.07	0.04	1.03	0.760	-81.65	-63.84
21	254.73	6.82	6.82	0.220	-99.10	-99.42

Table 2: Overall results of updating

After 300 iteration steps the iteration was stopped manually. From iteration step 206 to 207 the number of Monte Carlo samples was raised from 80 to 500 samples to stabilise the convergence of the covariance matrix. This results in a smoother convergence of the updating parameters since a higher sample size gives a better estimation of the sample space (see figure 2).

Table 2 shows the initial and updated frequency deviation for the mean frequency values and the according standard deviation. The *mean* and *std* value frequency deviations between test and analysis could be minimised quite well for the modes that have been used in the residual (1 to 6, 14 and 19). For the passive modes, nearly all frequency deviations of *mean* and *std* values get smaller, except for mode 11 and 12.

A graphical representation of initial and updated results is given in figure 8 and 9 where the results are illustrated as frequency clouds. In detail, figure 8 and 9 show the match of the test (blue) and analysis (red) scatter ellipses, which is also graphical representation of the two-dimensional frequency *covariance* matrix (see figure 1). The initial frequency clouds from test and analysis between f_2 and f_3 show a significant offset and a difference in orientation. After the updating process the distance and shape between these test and analysis clouds has nearly vanished which can also be observed for all other combinations concerning the modes used in the residual vector.

Figure 10 depicts the evolution of the updating parameters, the frequency deviations and MAC values over the iteration steps. This graph shows a nice parameter convergence. The raise of the sample size used for Monte Carlo Simulation smooths the convergence of the updating parameters for the *covariance* matrix. Overall, it can be observed that the mean values converge much faster than the covariance matrix values.

Nevertheless the final updating parameter correlation matrix, shown in figure 11b, seems to be a reasonable result. Here a very strong positive correlation was identified for pa-

rameter 5 and 6 which are both representing joint stiffness parameters at the HTP/VTP joint. On the contrary parameter 7, a mass parameter at the same location, shows a strong negative correlation to both previous mentioned parameters.

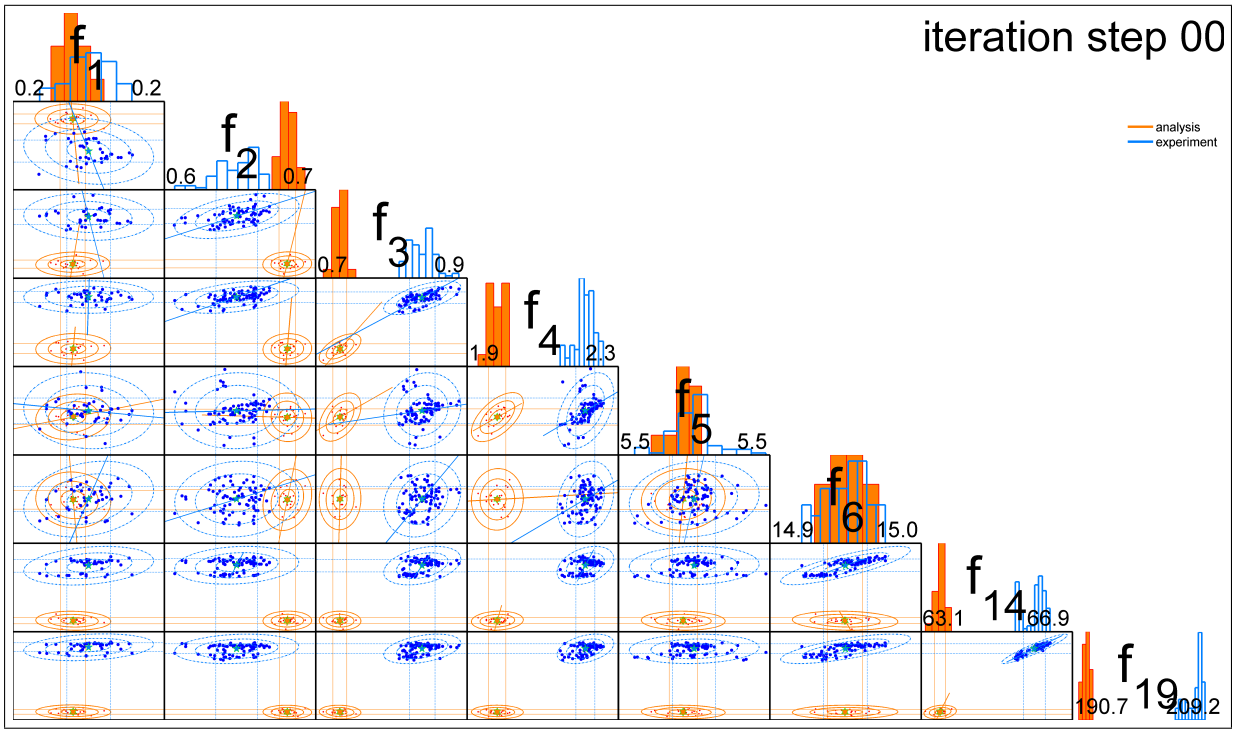

Figure 8: Frequency clouds used in residual before updating (test = blue, analysis = red)

6 CONCLUSIONS AND OUTLOOK

This paper describes how to perform stochastic model updating and how to establish uncertain experimental modal data. First, an overview was given about the impact of possible scatter sources (human operator, modal identification algorithm, measurement noise, structure variability due to production tolerances etc.) on modal data variability. After a classification of the influences, the final test database was derived from a structure by dis- and reassembling the bolted joint connections multiple times. The test data variability was observed in all modal parameters such as eigenfrequencies, damping, modal masses and mode shape amplitudes. An algorithm how to use uncertain modal test data for the identification of a stochastic finite element model has been introduced and successfully applied. The numerical uncertainty was derived by Monte Carlo Simulation using Latin Hypercube Sampling which demonstrates an efficient way of sampling. 500 samples were sufficient to yield a smooth convergence of the *covariance* residual for a number of eight updating parameters.

ACKNOWLEDGEMENTS

I am very grateful to Andrea Rode and Holger Haupt for doing so many modal tests in a row.

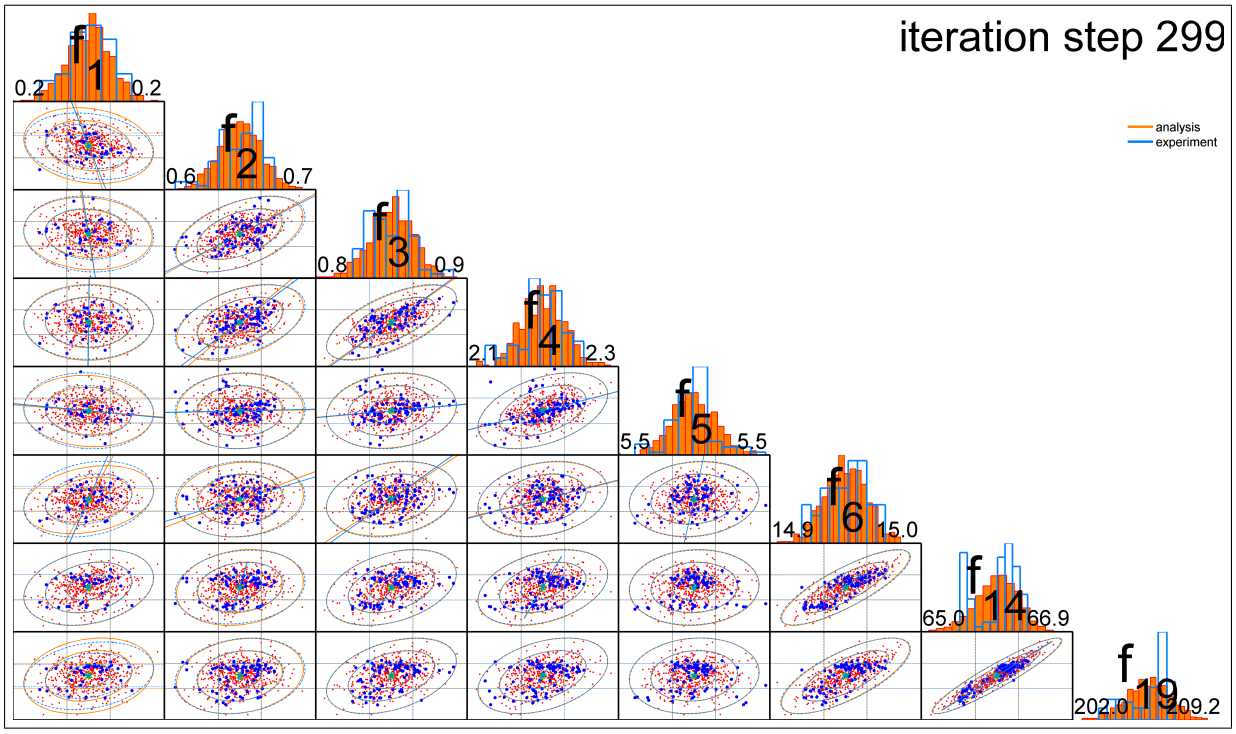

Figure 9: Frequency clouds used in residual after updating (test = blue, analysis = red)

7 REFERENCES

[1] Natke, H. (1992). *Einfuehrung in die Theorie und Praxis der Zeitreihen- und Modalanalyse*. Grundlagen und Fortschritte der Ingenieurwissenschaften. Braunschweig, Germany: Vieweg.

[2] Link, M. (1999). Updating of analytical models - basic procedures and extensions. In J. M. M. Silva and N. M. M. Maia (Eds.), *Modal Analysis and Testing*. Dordrecht, Netherlands: Kluwer Academic Publishers, pp. 281–304.

[3] Friswell, M. and Mottershead, J. (1995). *Finite element model updating in structural dynamics*. Solid mechanics and its applications, v. 38. Dordrecht; Boston: Kluwer Academic Publishers.

[4] Ladevze, P., Reynier, M., and Maia, N. (1994). Error on the constitutive relation in dynamics. In *Inverse Problems in Engineering Mechanics: Proceedings of the 2nd international symposium*. Paris, France: Taylor and Francis, pp. 251–256.

[5] Govers, Y., Boeswald, M., Goege, D., et al. (2006). Analysis of sources and quantification of uncertainty in experimental modal data. In P. Sas and M. De Munck (Eds.), *International Conference on Noise and Vibration Engineering*, vol. Proceedings of ISMA2006. KU Leuven, Belgium, pp. 4161–4173.

[6] Collins, J., Hart, G., Hasselman, T., et al. (1974). Statistical identification of structures. *AIAA Journal*, 12(2), 185–190.

[7] Mares, C., Mottershead, J., and Friswell, M. (2006). Stochastic model updating: Part 1 - theory and simulated example. *Mechanical Systems and Signal Processing*, 20(7), 1674–1695.

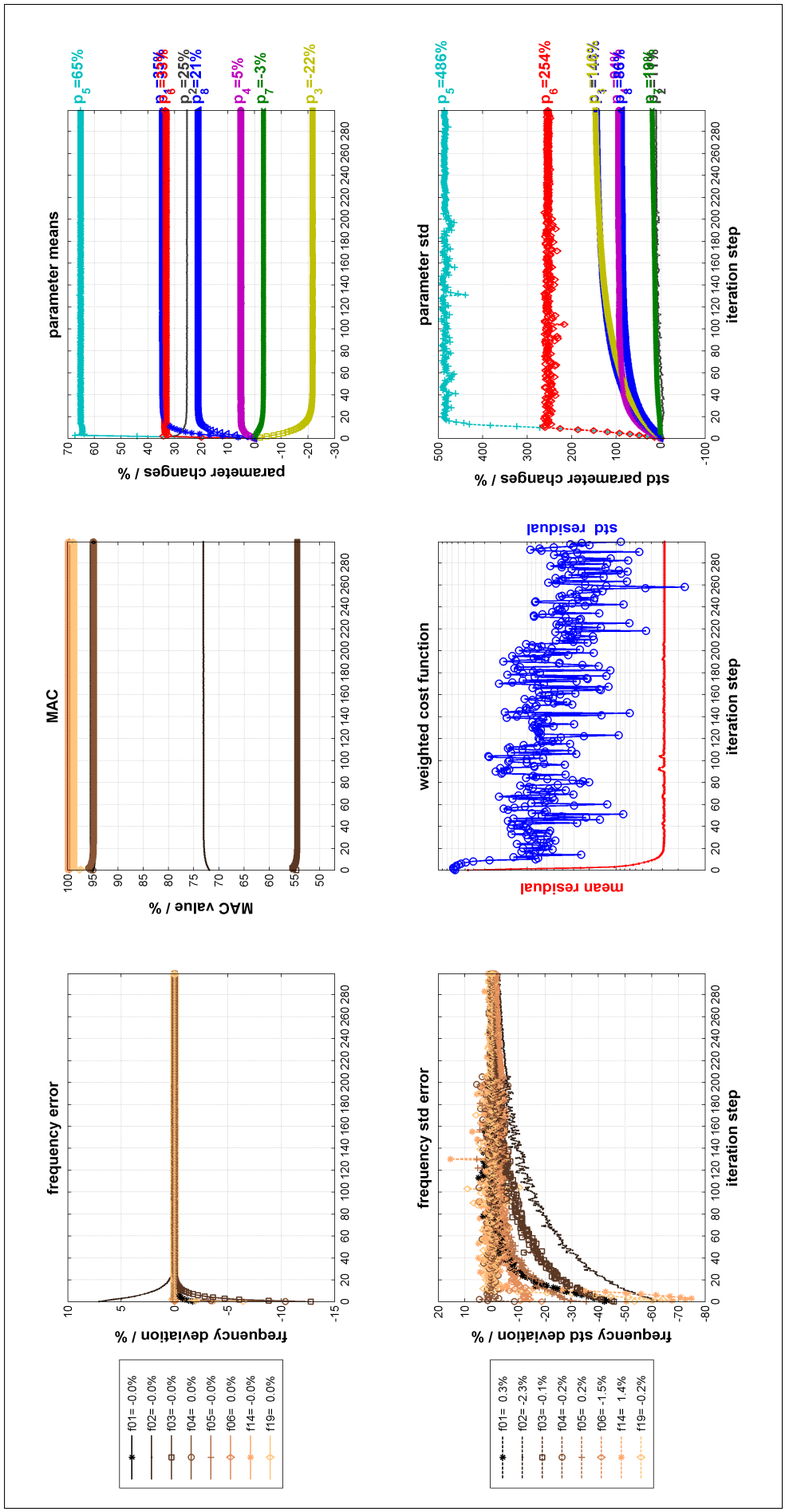

Figure 10: Evolution of frequency deviation, MAC values and update parameters

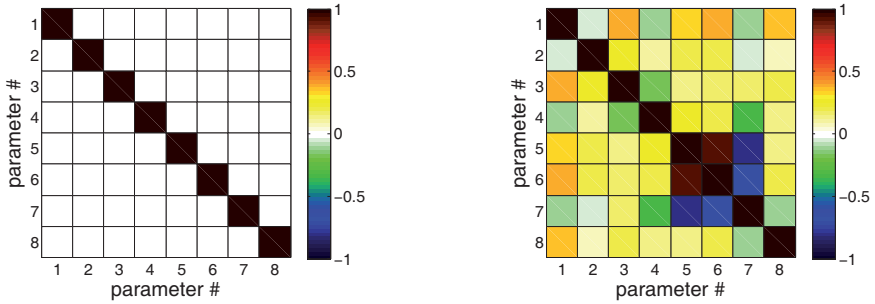

(a) before updating (b) after updating

Figure 11: Updating parameter correlation matrices

[8] Mottershead, J., Mares, C., James, S., et al. (2006). Stochastic model updating: Part 2 - application to a set of physical structures. *Mechanical Systems and Signal Processing*, 20(8), 2171–2185.

[9] Khodaparast, H., Mottershead, J., and Friswell, M. (2008). Perturbation methods for the estimation of parameter variability in stochastic model updating. *Mechanical Systems and Signal Processing*, 22(8), 1751–1773.

[10] Hua, X., Ni, Y., Chen, Z., et al. (2008). An improved perturbation method for stochastic finite element model updating. *International Journal for Numerical Methods in Engineering*, 73(13), 1845–1864.

[11] Khodaparast, H. H., Mottershead, J. E., and Badcock, K. J. (2011). Interval model updating with irreducible uncertainty using the kriging predictor. *Mechanical Systems and Signal Processing*, 25(4), 1204–1226. Doi: DOI: 10.1016/j.ymssp.2010.10.009.

[12] Govers, Y. and Link, M. (2010). Stochastic model updating – covariance matrix adjustment from uncertain experimental modal data. *Mechanical Systems and Signal Processing*, 24(3), 696–706.

[13] Govers, Y. and Link, M. (2009). Stochastic model updating by covariance matrix adjustment. In *Int. Conference on Structural Engineering Dynamics*, vol. ICEDyn2009. Ericeira, Portugal.

[14] Govers, Y. and Link, M. (2010). Stochastic model updating of an aircraft like structure by parameter covariance matrix adjustment. In P. Sas and B. Bergen (Eds.), *International Conference on Noise and Vibration Engineering*, vol. ISMA2010. KU Leuven, Belgium, pp. 2639–2656.

[15] Tikhonov, A. and Arsenin, V. (1977). *Solution of Ill-posed Problems*. Washington: Winston & Sons.

[16] Iman, R. L. and Conover, W. J. (1982). A distribution-free approach to inducing rank correlation among input variables. *Communications in Statistics - Simulation and Computation*, 11(3), 23.

[17] Balmes, E. (1997). Garteur group on ground vibration testing. results from the test of a single structure by 12 laboratories in europe. In *International Modal Analysis Conference*, vol. 15. Orlando, Florida, USA, pp. 1346–1352.

[18] Degener, M. (1997). Ground vibration tests on an aircraft model performed as part of a european round robin exercise. In *International Forum on Aeroelasticity and Structural Dynamics*. Rome, Italy, pp. 255–262.

[19] Balmes, E. (1998). Predicted variability and differences between tests of a single structure. In *International Modal Analysis Conference*, vol. 16. Santa Barbara, California, USA, pp. 558–564.

[20] Link, M. and Friswell, M. (2003). Working group 1: Generation of validated structural dynamic models–results of a benchmark study utilising the GARTEUR SM-AG19 test-bed. *Mechanical Systems and Signal Processing*, 17(1), 9–20. ISSN 0888-3270. doi:DOI: 10.1006/mssp.2002.1534.

[21] Guillaume, P., Verboven, P., Vanlanduit, S., et al. (2003). A poly-reference implementation of the least squares complex frequency-domain estimator. In *International Modal Analysis Conference*, vol. 21. Kissimmee, FL, USA.

[22] Govers, Y., Boeswald, M., and Goege, D. (2007). Quantification and error source classification of uncertainty in experimental modal data supported by stochastic finite element analysis. In *Onera DLR Aerospace Symposium*, vol. Proceedings of ODAS2007. Göttingen, Germany.

[23] Heylen, W., Lammens, S., and Sas, P. (1998). *Modal Analysis Theory and Testing*. Leuven: KU Leuven.

[24] Allemang, R. and Brown, D. (1982). A correlation coefficient for modal vector analysis. In *International Modal Analysis Conference*, vol. 1. Orlando, FL, USA, pp. 110–116.